

Production of K X Rays by 160-MeV Protons

O. N. Jarvis and C. Whitehead

Atomic Energy Research Establishment, Harwell, Berkshire, United Kingdom

and

M. Shah

Department of Physics, University of Surrey, Guildford, United Kingdom

(Received 22 September 1971)

K -shell ionization cross sections have been measured for elements between $Z=26$ and $Z=92$ using 160-MeV protons as incident projectiles. The results are compared with two theoretical models, the plane-wave-Born-approximation calculations of Khandelwal, Choi, and Merzbacher and the binary-encounter model of Garcia. The results are in qualitative agreement with both these nonrelativistic models. The necessity for a relativistic theory is emphasized by comparison with recent high-energy-electron measurements.

I. INTRODUCTION

Many experimental and theoretical studies have been made of the production of K x radiation from various materials by heavy particles of very low energy. The early work in this field was reviewed by Merzbacher and Lewis¹ in 1958. Until very recently, subsequent work² was also concerned with low-energy projectiles. When the present work was initiated the most recent experimental study was that of Sellers *et al.*,³ who used α particles in the energy range 1–5 MeV. During the course of the present work, however, further measurements have become available including those of Bissinger *et al.*⁴ using 2–28-MeV protons, and of Richard *et al.*⁵ using 6–10-MeV protons and 15–19-MeV oxygen ions. Of particular related interest are the ultrarelativistic electron measurements of Middleman *et al.*⁶ using electrons in the range 150–900 MeV.

Previous to the present work all the heavy particle K x-radiation cross-section data have been obtained at quite low projectile energies for which a nonrelativistic theoretical treatment is expected to be reasonably accurate. A major incentive for the present measurements was to extend the proton work to high energies in order to investigate the importance of relativistic effects. In particular, it was of interest to test whether the production cross section, which was expected to rise to a maximum for a proton velocity close to the rms velocity of the K -shell electron, would indeed fall as $1/E$ on the high-energy side of the peak as predicted. The present high bombarding energy readily permits a study of the excitation cross sections for even the heaviest stable elements. This is in contrast with the other recent measurements^{2–5} in which only light elements ($Z \leq 29$) were studied. Whereas previous work has usually been for a single element as a function of energy, the present work

is for a wide range of elements at a single energy—a consequence of the type of particle accelerator used. According to the existing nonrelativistic theories the two different approaches provide equivalent results.

II. EXPERIMENTAL ARRANGEMENT

The experimental geometry is shown in Fig. 1. The 160-MeV proton beam from the Harwell synchrocyclotron was focused onto the targets by three pairs of quadrupoles to form a spot of about 1 cm diam over-all. After emerging from the evacuated target chamber the proton beam first passed through a 1-mm-thick sheet of polythene used as a target for a p - $2p$ intensity monitor and was then collected in a 10-cm-diam Faraday cup for normalization purposes. The target chamber was constructed so that the target foils were observed by the x-ray detector at a scattering angle of 155° to the beam direction. This large angle was required to reduce the intensity of high-energy protons scattered by the target which might subsequently pass through the detector.

The x-ray detector was a Si(Li) detector of 1.10-cm² area and 5 mm thick. The energy resolution was 1.3 keV at 6 keV, which was quite adequate for the present work. Si(Li) was chosen instead of Ge(Li) because the narrow region of energy sensitivity of the Si(Li) detector is desirable when used in regions of very high background radiation levels, such as exist in the experimental areas of the synchrocyclotron.

The amplified signals from the Si(Li) detector were fed into an ADC coupled to the on-line Honeywell DDP-516 computer using the standard CAMAC interface electronics.⁷ The computer was used in multiprogramming mode so that the software permitted data reduction, graph plotting, and magnetic tape data storage and retrieval, all to be carried on simultaneously with data acquisition. Typical

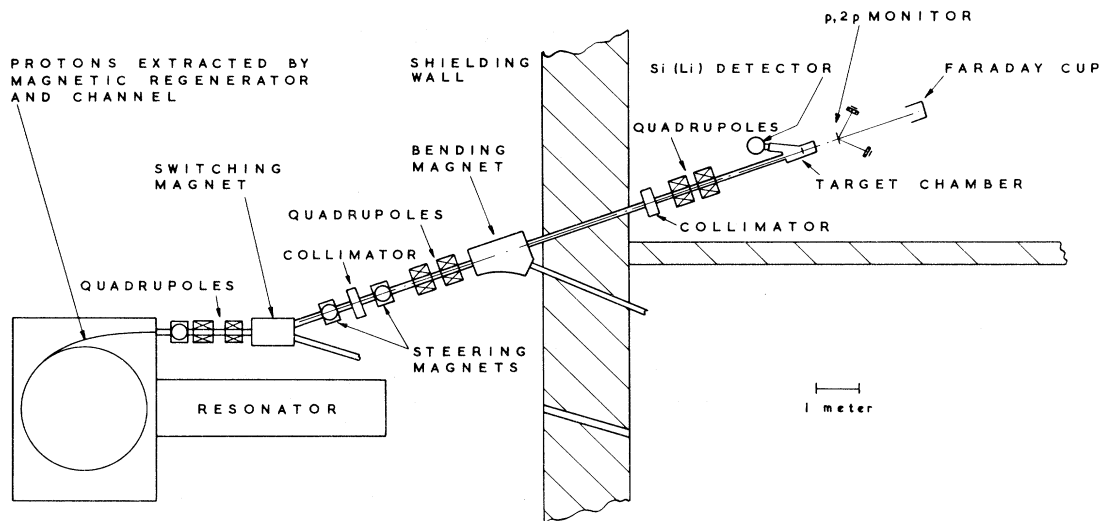


FIG. 1. General layout of the machine and experimental area.

pulse-height spectra are shown in Fig. 2. Counting rates were generally in the range 500–5,000 counts/sec, using beam currents of between 0.3 and 3.0 nA. The normal duty cycle of the beam extracted from the synchrocyclotron was increased to about 20% with the use of the auxiliary Cee electrode,⁸ but nevertheless the dead-time corrections were large (5–50%) and their determination was a major problem. To enable dead-time corrections to be made, a pulser was fed both into the detector preamplifier and into a separate scaling system. To allow for the pulsed nature of the proton beam, this pulser was triggered by signals from the p - $2p$ monitor. However, corrections based on this technique were not entirely satisfactory, presumably because the duty cycle for the characteristic x rays is different from that for the backgrounds (which arise from long life induced activity) and consequently measurements were made at several beam levels so that an extrapolation to zero count rate could be made for each target. Additional complications arose from the fact that the effective duty cycle of the beam varied with time and with beam level. Use of very low beam levels to minimize counting losses was impracticable owing to the difficulty of integrating accurately beam currents below 0.1 nA.

A consequence of the high background in the experimental area was the necessity to use thick targets; the target thickness used lay in the range 1–200 mg/cm². Corrections were made for the absorption by the target of its own characteristic K x radiation. The use of thick targets also introduced the need to allow for the subsidiary effect of characteristic K x radiation produced by the energetic δ rays which in turn are produced by the incident protons whilst passing through the target. This contribution was taken into account by making mea-

surements for each element as a function of target thickness. Some care was necessary in the extrapolation to zero thickness because the δ -ray contribution is not linear with thickness, and only in the limits of very thin or very thick targets is a linear dependence obtained; in the latter case the extrapolation to zero thickness does not give the desired cross section. The two limiting regions occur because the δ -ray contribution arises from two distinct physical processes. For very thin targets only the direct ionization by the δ ray is important, but for thick targets the secondary process involving bremsstrahlung production followed by photoelectric absorption provides an important contribution. In the Appendix the results of approximate calculations of the apparent ionization cross sections due to these processes are compared with experiment. Where necessary, these calculations were used to guide the extrapolation of the experimental cross sections to zero target thickness.

Except for the two elements Ba and Tb, the targets were all in the form of self-supporting metal foils. The two exceptions were provided in the form of the oxides painted onto a hydrocarbon backing. Target thicknesses were estimated both by weighing and by measurements of x-ray attenuations using appropriate radioisotope sources and the convenient tabulation of absorption coefficients of Dewey *et al.*⁹ Since the accuracy of the coefficients presented in this tabulation is expected to be only $\pm 5\%$ on average, the attenuations were measured for several different photon energies. A generous uncertainty of $\pm 3\%$ was attributed to the target thickness measurements for the self-supporting foils, but the much larger uncertainty of $\pm 20\%$ was attributed to the two oxide targets as these were noticeably nonuniform.

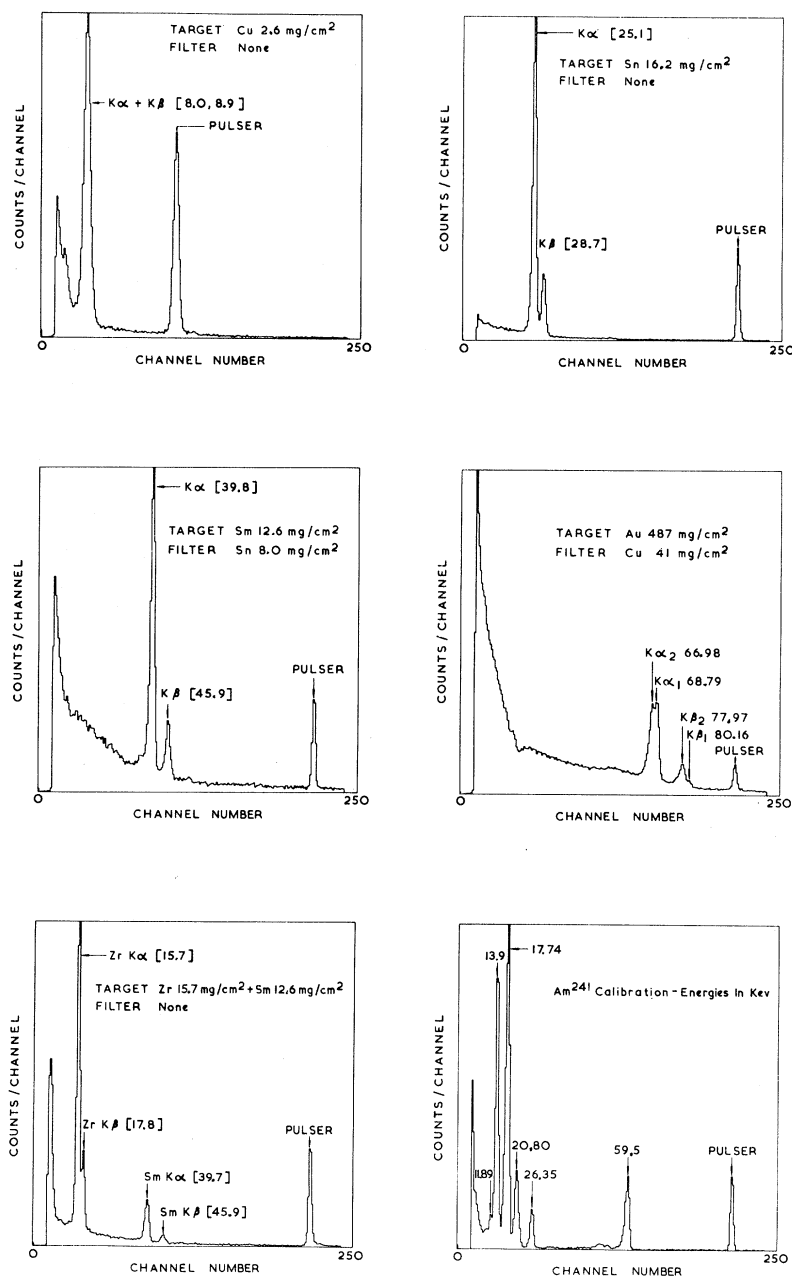


FIG. 2. Typical pulse-height spectra of the characteristic x radiation produced by bombardment with 160-MeV protons.

The detector efficiency was determined over the energy range 6–120 keV using radioisotope sources of ^{241}Am , ^{160}Tb , and ^{57}Co assuming the relative γ -ray yields quoted by Lederer *et al.*¹⁰ and the $x:\gamma$ yield for ^{57}Co given by Campbell *et al.*¹¹ The shape of the low-energy side of the efficiency curve near the 6.4-keV ^{57}Co line was obtained by calculation from the known materials of the cryostat windows and the assumption that any residual loss of efficiency at 6.4 keV was attributable to a Si dead layer on the front surface of the detector. The active area of the detector was determined using an ^{55}Fe

source and a collimator of known dimensions. Interpolated efficiencies for each target element are given in Table I.

III. EXPERIMENTAL MEASUREMENTS

The experimental measurements were spread over three separate data-taking periods, with much repetition. For each element at least two separate targets were used. For the heavier elements Ta through U it was necessary to interpose an appropriate filter between the target and detector to absorb preferentially the highly intense L x radiation.

TABLE I. The total ionization cross sections for each target element, together with the assumed fluorescent yields and detector efficiencies. Over-all accuracy: $\pm 7\%$. σ_K = total K-shell ionization cross section assuming isotropic emission. η = interpolated detector efficiency. ω_K = fluorescent yield (Ref. 10) assumed in deducing σ_K ; no allowance has been made for uncertainties in ω_K .

Element	Z	Target thickness range (mg/cm ²)	ω_K	η	σ_K (b)
Fe	26	1-3	0.293	0.36 \pm 0.03	780 \pm 65
Cu	29	2.5-41.1	0.393	0.62 \pm 0.04	560 \pm 40
Zr	40	5.5-16.0	0.70	0.89 \pm 0.02	193 \pm 13
Mo	42	2.8-52.0	0.73	0.88 \pm 0.02	162 \pm 7
Rh	45	5.8-16.4	0.78	0.81 \pm 0.03	149 \pm 7
Ag	47	7.7-23.3	0.80	0.76 \pm 0.03	136 \pm 7
Sn	50	8.0-24.2	0.84	0.68 \pm 0.03	112 \pm 6
Ba	56	7.0-21.0	0.88	0.52 \pm 0.02	48 \pm 10
Sm	62	10.0-55.0	0.91	0.35 \pm 0.02	50 \pm 2.8
Tb	65	9.8	0.92	0.27 \pm 0.02	32 \pm 6
Ta	73	91.7-185.9	0.94	0.132 \pm 0.008	24.3 \pm 1.6
Pt	78	22.5	0.95	0.083 \pm 0.005	19.2 \pm 1.4
Au	79	2.7-487.2	0.95	0.076 \pm 0.004	17.7 \pm 1.0
Pb	82	25-75	0.96	0.059 \pm 0.005	19.2 \pm 1.7
U	92	207	0.96	0.027 \pm 0.005	10.5 \pm 1.9

This introduced only a small correction for absorption of the K x rays.

For all the elements except Fe and Cu the photopeak intensities were extracted from the spectra assuming a linear background dependence. For the two light elements this was inapplicable and the background was estimated by eye; fortunately, the necessary background subtractions were small. Some difficulty was experienced in subtracting the background from the spectra for the thinnest gold target (2 mg/cm²) and for the uranium target (207 mg/cm²). The difficulty for uranium was partly due to the small cross section, to the high background, and to the $K\alpha_1$ and $K\alpha_2$ radiations being sufficiently separated as to reduce the apparent cross section relative to the lighter targets for which these two radiations were not resolved. It is pertinent to note that the cross section for production of K x rays from uranium is comparable with the cross section for induced fission.

For elements with atomic number below 65 both $K\alpha$ and $K\beta$ radiations were summed together, but for elements with $Z \geq 65$ only the $K\alpha$ contribution was taken from the spectra and the $K\beta$ contribution was estimated from the known $K\beta:K\alpha$ ratios as obtained from x-ray fluorescence studies.¹²

It was assumed implicitly in the present experiment that the emission of characteristic K x radiation is isotropic. This point has been investigated and found valid by Merzbacher and Lewis¹ for L x rays from gold and was again checked in the high-energy-electron measurements of Middleman *et al.*⁶

The final K-shell ionization cross-section data are listed in Table I, together with the assumed fluorescent yields¹⁰ and the detector efficiency. There is an over-all normalization uncertainty to be ap-

plied to these data. This uncertainty contains contributions from the detector sensitive area, the solid angle subtended at the target, the Faraday-cup calibration, and for the collection of δ rays in the Faraday cup—these δ rays being produced in the window of the Faraday-cup vacuum chamber. Summing these contributions quadratically yields an over-all uncertainty of $\pm 7\%$.

Some preliminary measurements were also made using the 85-MeV deuteron and the 160-MeV α -particle beams from the synchrocyclotron. These measurements were bedevilled by counting rate and dead-time problems because the long duty-cycle facility exists only for the proton beam.

IV. RESULTS

A. Proton Data

The final cross-section data for 160-MeV protons are listed in Table I and are presented graphically in Fig. 3. The solid curve is derived from the plane-wave-Born-approximation (PWBA) calculations conveniently tabulated by Khandelwal *et al.*¹³ These calculations were made for low-energy pro-

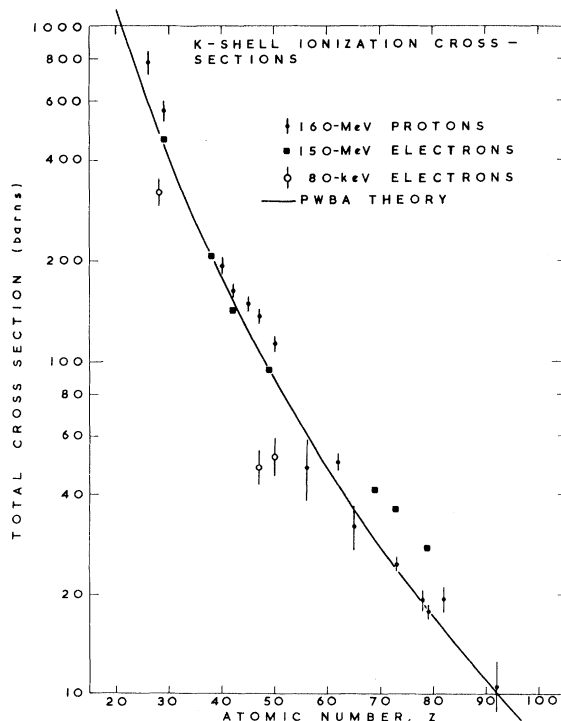


FIG. 3. Total K-shell ionization cross sections for a range of elements between $Z=26$ and $Z=92$. The 160-MeV proton data are compared with a PWBA theory (which has been scaled by a factor of 1.26, see text). The data are compared with results for electrons of the same velocity as the protons (80-keV electrons) and with results for 150-MeV electrons (for which the agreement with PWBA theory is entirely fortuitous).

jectiles and utilized nonrelativistic hydrogenic wave functions for the atomic states. The total cross section σ_K is expressed as

$$\sigma_K = (8\pi z^2 a_0^2 / Z_K^4 \eta_K) f_K(\eta_K, \theta_K).$$

In this expression ze is the projectile charge, $Z_K e$ is the effective nuclear charge as seen by a K -shell electron, and a_0 is the Bohr radius of hydrogen. The quantity η_K is dimensionless and is given by

$$\eta_K = mE / MZ_K^2 R_\infty,$$

where m is the electron mass, M and E are the mass and energy of the incident particles, and R_∞ is the Rydberg constant (13.605 eV). Finally, $f_K(\eta_K, \theta_K)$ is the quantity which is actually tabulated by Khandelwal *et al.* The parameter θ_K is the K -shell screening number

$$\theta_K = \epsilon_K / Z_K^2 R_\infty \approx 1,$$

where ϵ_K is the observed K -shell ionization potential; θ_K is the lower limit of the integration defining f_K . The effective charge is taken to be $Z_K = Z - 0.3$, as is customary. Rather than use the θ_K values computed from the simple relationship above, we adopt the values given by Walske¹⁴ where θ_K has been modified so as to partially correct for the relativistic contributions to the binding energy ϵ_K . In Fig. 3 the theoretical PWBA curve has been multiplied by the factor 1.26 in an attempt to correct at least partially for the relativistic velocity of the 160-MeV protons. It is assumed that the most important kinematic factor in the PWBA formula for

σ_K is the $1/v^2$ term which enters through the ratio M/E contained in the quantity η_K . The impulse approximation calculation—to be discussed later—also possesses such a factor. It is clearly desirable to use the true relativistic velocity in the $1/v^2$ term instead of the velocity computed using nonrelativistic kinematics, hence the factor 1.26. This correction factor is by no means sufficient compensation for not using relativistic kinematics throughout but perhaps gives a fair estimate of the magnitude of the corrections required at the present energy. Furthermore, as the energy moves into the highly relativistic region, σ_K will begin to increase because of the relativistic enhancement of the transverse component of the electromagnetic field.

The “theoretical” curve in Fig. 3 provides a good qualitative description of the data. Perhaps surprisingly, the fit is best for high- Z elements where the lack of a relativistic description for the atomic states would have been thought most serious. Figure 3 also presents some K -shell ionization data obtained for electrons: These data will be considered later.

In Fig. 4 we again present the ionization data for 160-MeV protons, but this time in a form which permits comparison with data for other heavy projectiles taken over a wide range of energies. Merzbacher and Lewis¹ have shown that there is an approximate relationship

$$f_K(\eta_K, \theta_K) \approx \theta_K f_K(\eta_K / \theta_K^2, 1).$$

Since this enables us to write

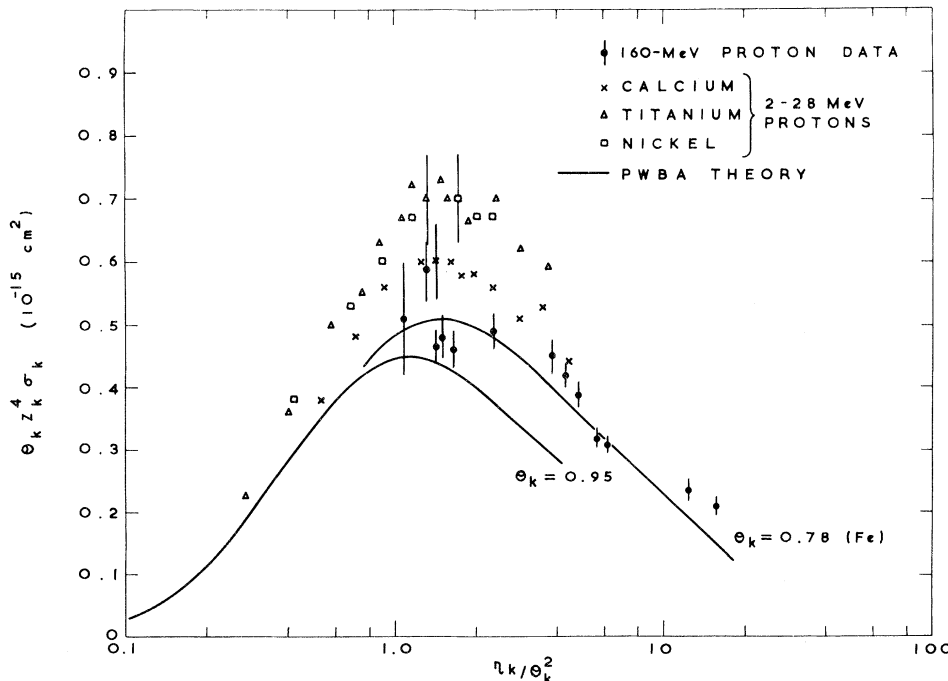


FIG. 4. Comparison of the high-energy proton-induced cross-section data with PWBA theory in the form of the “universal curve” of Merzbacher and Lewis. Note that the 2–28-MeV data of Bis-singer *et al.* (Ref. 4) are for three selected elements as a function of energy, whereas the 160-MeV proton data are for a range of elements at a single energy. (The 160-MeV data have been reduced by the factor 1.26, see text).

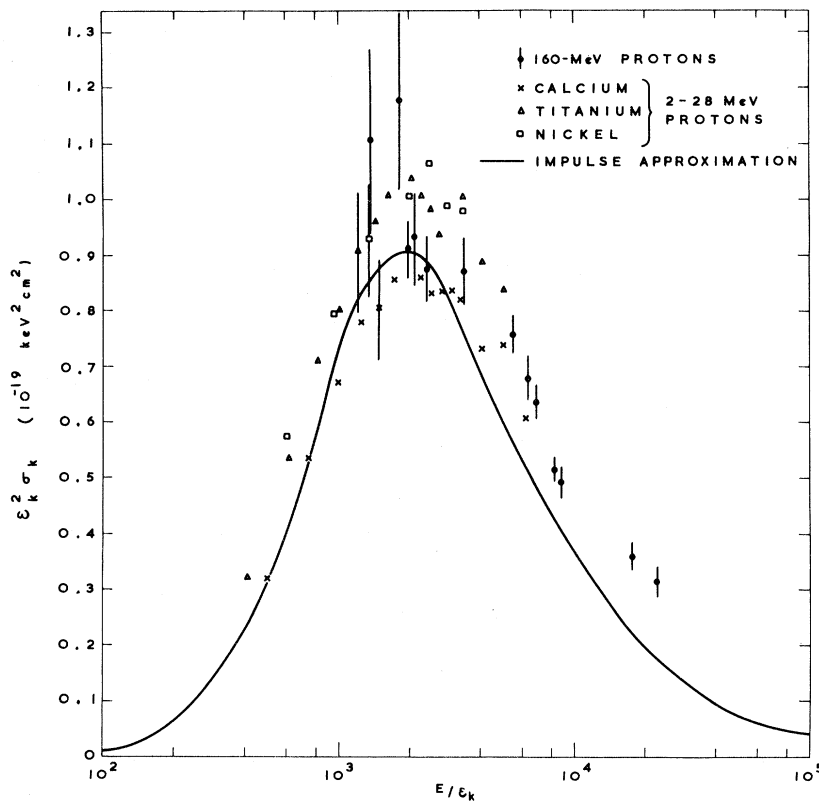


FIG. 5. Comparison of the high-energy proton-induced cross-section data with the binary-encounter model of Garcia. (The 160-MeV data have been reduced by the factor 1.26, see text.)

$$\theta_K Z_K^4 \sigma_K / z^2 \approx 8\pi a_0^2 (\theta_K^2 / \eta_K) f_K(\eta_K / \theta_K^2, 1),$$

we see that a “universal” curve can be obtained by plotting $\theta_K Z_K^4 \sigma_K / z^2$ against η_K / θ_K^2 . This approximation is quite good on the low-energy side of the maximum, where existing data for energies such that the abscissa lies between 0.005 and 1.0 cover six orders of magnitude of the ordinate. However, it does not hold very well for the high-energy side of the maximum as can be seen (Fig. 4) by the differing results for $\theta_K = 0.78$ and $\theta_K = 0.95$. In this presentation the 160-MeV proton data have been scaled for the effect of relativity, instead of the theoretical curves. (Also, in this and later figures, the data for the two oxide targets have been omitted as their uncertainties are large and tend to obscure other pertinent features.) Shown together with the 160-MeV data for Z between 26 and 92 are the 2–28-MeV proton data of Bissinger *et al.*⁴ for Ca, Ti, and Ni. It is clear that the fit of theory to experiment is poorer for the low-energy proton data than for the 160-MeV data. In fact, the PWBA theory underestimates the Ti and Ni data by about 50%. Perhaps it should be noted that the absolute errors on the low-energy data are quite large (11–13%) and that for relatively light elements such as Ca, Ti and even Ni there is a possibility that the fluorescent yields may be substantially in error.

A simpler method of presenting K -shell ionization data has been proposed by Garcia.¹⁵ He has shown that a classical binary-encounter model¹⁶ (an impulse-approximation calculation) provides a very simple scaling law such that $\epsilon_K^2 \sigma_K$ plotted against E/ϵ_K defines a universal function. Such a graph is more convenient than the PWBA method which involves the parameters η_K and θ_K . Moreover, this impulse-approximation calculation provides a better fit¹⁶ to the low-energy data ($\eta_K < 1$ or $E/\epsilon_K < 2000$). Figure 5 presents the proton data (modified, as before, for relativistic projectiles) on a graph drawn to Garcia’s prescription. It is clear that this representation is more truly universal than that provided by the PWBA calculation, that the fit to the 160-MeV data is of similar quality to that shown in Fig. 3 and, furthermore, that the fit to the 2–28-MeV data is now greatly improved.

B. Deuteron and α -Particle Data

As mentioned earlier, these results are of a preliminary nature. Therefore, we restrict ourselves to considering only the averaged results for five elements between $Z = 29$ and $Z = 79$, expressed as ratios for the different projectiles. The comparison between the 160-MeV α particle and the 85-MeV deuteron data is particularly simple because

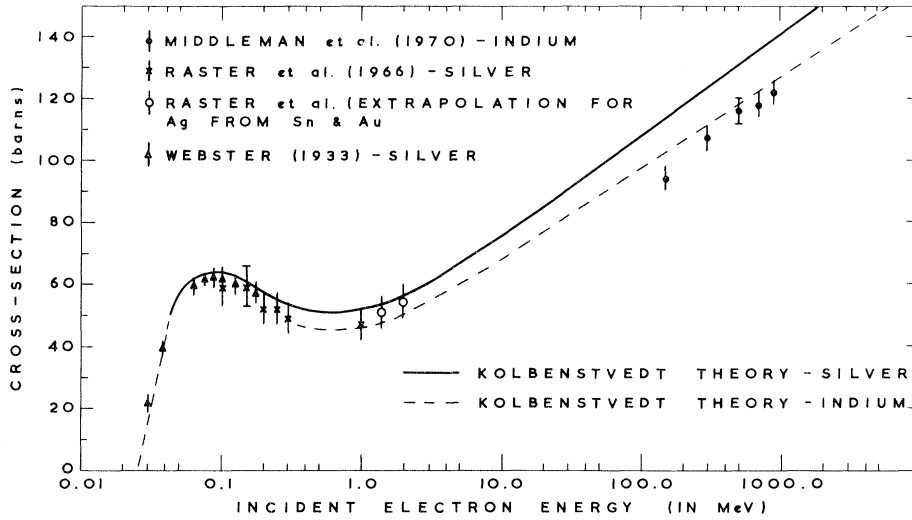


FIG. 6. Total K-shell ionization cross sections for indium and silver using electrons as incident projectiles, as a function of electron energy. Comparison is made with the theory of Kolbenstvedt (Ref. 17).

the velocities of these two projectiles are equal—the theoretical ratio for each element is then just 4/1, arising from the fact that the α particle possesses charge $z=2$. Experimentally, we have observed a mean ratio of 4.6 ± 0.8 . For the ratio of α particle to proton cross-section data the situation is more complicated because the projectile velocities are quite different. Following the PWBA theory, the α -particle cross section is enhanced relative to the proton cross section by a factor of 4 through the factor z^2 , a further factor of 4 (non-relativistically) for the reduction in η_K and is reduced by an amount dependent on Z through the factor f_K . It was found that the experimental ratio $\sigma_K(\alpha)/\sigma_K(p)$, divided by the theoretical ratio, taken

as an average for all Z was 0.96 ± 0.10 . Since good qualitative agreement has already been demonstrated for the proton data with theory, this result indicates that the α -particle data (and, from the previous result, the deuteron data also) are in equally good agreement with theory.

V. COMPARISON WITH ELECTRON DATA

In any first-order theory of the interaction between a very fast charged particle and an atomic electron, the ionization cross section will be determined essentially by the atomic number of the target atom, the magnitude of the projectile charge, and its velocity, but should be relatively independent of the projectile mass. This is not true, of

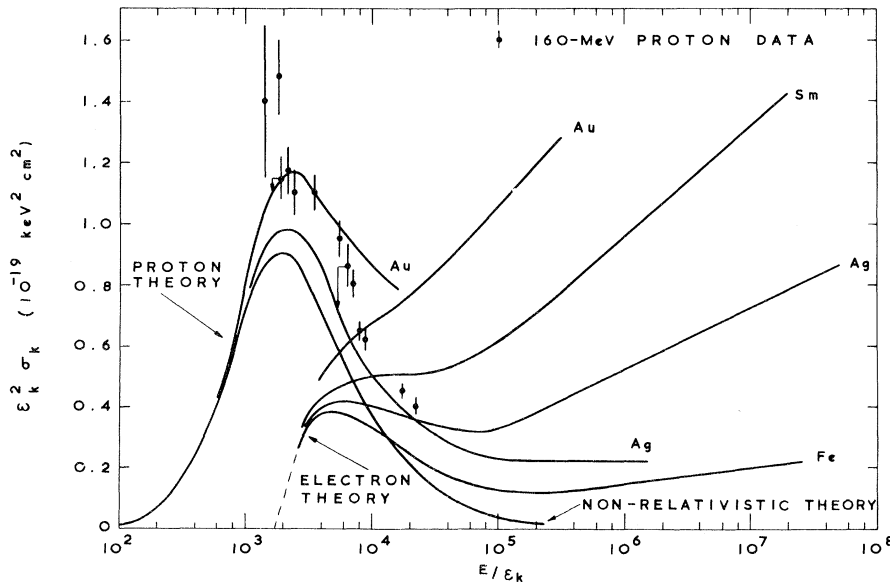


FIG. 7. An attempt to predict the variation of the proton-induced total K-shell ionization cross sections in the highly relativistic energy region.

course, for low projectile velocities where the various conservation laws impose kinematic restrictions which in turn define the low-energy behavior of the cross sections. For low-energy electrons the increase in kinetic energy experienced by the electron while penetrating the atom is most important, and the energy threshold for ionization is determined solely by energy conservation. For protons a purely two-body collision would imply a threshold velocity one-half that for electrons but, in fact, the proton production of K -shell ionization is appreciable for energies considerably less than this because the internal motion of the atomic electron is important (momentum conservation being satisfied by the recoil of the atom).

For proton energies well above the "classical" threshold of approximately $460\epsilon_K$, we would expect proton- and electron-produced ionization cross sections to be equal provided the projectile velocities are the same. We therefore compare the present 160-MeV proton data with 80-keV electron data. Very few electron measurements have been made, and Fig. 3 presents the only available data (for Ni, Ag, and Sn). That these electron data are smaller than the proton data is not surprising, since we really require data for elements of very low Z for which the electron-production cross sections are determined by momentum conservation rather than energy conservation. However, the electron and proton data appear to be converging as Z decreases.

Also shown in Fig. 3 are the 150-MeV electron data of Middleman *et al.*,⁶ the three high- Z points being extrapolated downwards from their 300–900-MeV data. The remarkable agreement with our 160-MeV proton data is entirely fortuitous. The variation with Z for electrons is a good fit to Z^{-n} with $n = 2.70 \pm 0.02$. The proton data does not possess such a simple Z dependence, but for comparison purposes a reasonable representation can be found with $n \approx 3.3$.

The behavior of the electron data for Ag with energy is shown in Fig. 6. This figure covers an energy range from 25 keV to 900 MeV, and clearly the fit to the revised relativistic theory of Kolbenstvedt¹⁷ is excellent. For the nonrelativistic energy range the cross sections may be expressed¹⁸ as

$$\epsilon_K^2 \sigma_K = 7.92 \times 10^{-20} (\epsilon_K/E) \ln E / \epsilon_K \text{ cm}^2 \text{keV}^2.$$

This relationship provides a "universal" curve bearing a very strong resemblance to the prescription of Garcia.¹⁵

We expect the cross-section data to be similar for protons and electrons at the same velocity when in the ultrarelativistic energy region. (The cross sections cannot be identical since the proton and electron magnetic moments differ.) Figure 7 has been drawn in an attempt to gain some feeling for the behavior of the proton data in the relativistic

energy region. This figure should be viewed not as an attempt to provide a universal curve for all Z at any energy, as previously considered, but rather as an indication of the energy dependence for each particular element. The curves labelled "electron theory" have been adapted from the theory of Kolbenstvedt by the simple expedient of using as the abscissa the proton energy corresponding to the same velocity of the electron to which the Kolbenstvedt theory applies. The three "proton theory" curves are adapted from the theory of Garcia *et al.*¹⁶; of these three curves one is the uncorrected theory and the other two—for Ag and Au—being obtained by making the approximate correction for projectiles of relativistic velocities as before. The collapse of the "universal" curve and the expected crossover of the true cross sections from the behavior given by the nonrelativistic proton theory to that of the relativistic electron theory can be readily imagined.

VI. CONCLUSIONS

Cross sections for the K -shell ionization produced by 160-MeV protons have been measured for elements in the range $26 \leq Z \leq 92$. These cross sections have been shown to be in qualitative agreement with both the PWBA calculations of Khandelwal *et al.*¹³ and the binary-collision model calculations of Garcia *et al.*,¹⁶ provided approximate correction is made for the relativistic velocity of the protons. For lower energies the binary-collision model provides a better fit to the data than the PWBA method and any existing discrepancies between this theory and the low-energy experiments are as likely to be due to uncertainties in the various experimental measurements as to the approximation of the theory. Preliminary measurements with 85-MeV deuterons and with 160-MeV α particles have also been found to be in good agreement with theory.

Attention has been given to the manner in which the proton cross sections vary with energy as the energy moves into the relativistic region. The nonrelativistic theories are clearly on the verge of breaking down at 160 MeV. The need for a fully relativistic proton theory is therefore apparent. Since the Kolbenstvedt theory fits the ultrarelativistic electron data remarkably well without recourse to a relativistic description of the atomic wave functions, it is probable that this complication will also prove unnecessary for the proton work.

ACKNOWLEDGMENTS

The authors are particularly grateful to C. G. Clayton for stimulating their interest in this problem. They are also very grateful to A. C. Sherwood for his assistance in the preparation for and execution of the data taking and to the cyclotron crew for their efficient running of the machine.

APPENDIX: CORRECTIONS FOR SECONDARY K X-RAY PRODUCTION PROCESSES

In the study of K -shell ionization by heavy ions of high energy, there are competing ionization processes which must be considered. These processes are due to the copious production of δ rays of sufficient energy to eject K -shell electrons either in direct collisions or indirectly by photoelectric absorption of the bremsstrahlung radiation associated with the δ rays. This radiation arises both from the slowing down of the δ rays in the target and from the initial impacts in which the δ rays are formed.

Ideally, difficulties arising from these secondary ionization processes would be avoided by the use of extremely thin targets. However, when relatively thick targets are required—as in the present experiment—it becomes necessary to measure the excitation cross section as a function of target thickness and to extrapolate to zero thickness. Some approximate calculations¹⁹ were made to discover the range of target thickness over which a linear extrapolation could be considered appropriate. The calculations were made for the two extreme cases: (a) In the thin-target approximation the δ rays pass through the target without loss of energy. (b) In the thick-target approximation the δ rays are all stopped within the target medium.

Two further gross simplifications were made by assuming (i) the bremsstrahlung radiation is either isotropic, or (ii) the bremsstrahlung radiation is strongly peaked in the forward direction. The forward-peaking assumption is reasonable for very high-energy δ rays, but the isotropic production may be more appropriate to very low-energy δ rays. However, low-energy δ rays can contribute only to the ionization of low- Z elements for which the bremsstrahlung process is relatively unimportant. Consequently we expect the forward-peaking or “relativistic” approximation to be more realistic than the “isotropic” approximation.

In Fig. 8 we show the experimentally determined K -shell ionization cross sections for 160-MeV protons on copper and gold as a function of target thickness. These data have been corrected for self-absorption of the K x radiation in the targets. The discontinuities in the curves indicate the change

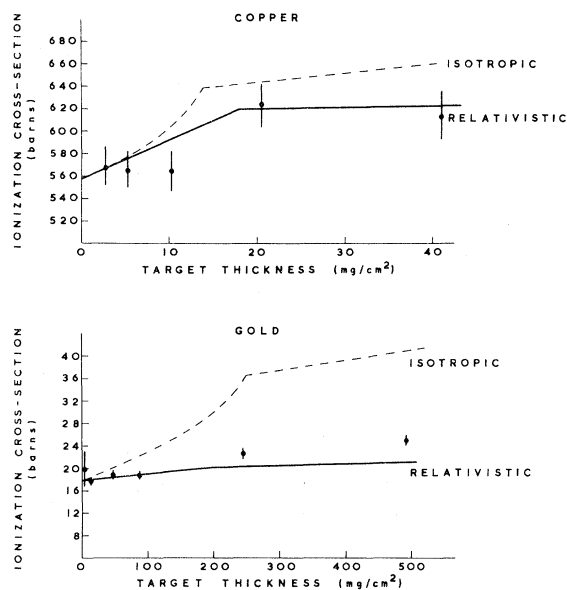


FIG. 8. Apparent K -shell ionization cross sections for copper and gold, measured as a function of target thickness.

from the “thin” to the “thick” target approximations. For copper the “isotropic” and “relativistic” calculations give very similar results, a reflection of the insignificance of the indirect (bremsstrahlung production) process relative to the direct collision process for low- Z elements. The copper data clearly favor the “relativistic” calculations. For gold the difference between the “isotropic” and “relativistic” calculations is very considerable, but—again, as expected—the data strongly favor the relativistic calculations. From these two comparisons we conclude that the “relativistic” calculations may be used to make surprisingly precise corrections for the δ -ray ionization processes and this, in turn, implies that the limiting factor in choice of target thickness need not be an awareness of the δ -ray ionization process but simply the desire to keep the self-absorption corrections to acceptably small values. For most of the measurements in the present work the magnitude of the δ -ray ionization corrections are less than the uncertainties in target thickness.

¹E. Merzbacher and H. Lewis, in *Encyclopedia of Physics*, edited by S. Flügge (Springer-Verlag, Berlin, 1958), Vol. 34, p. 166.

²R. R. Hart, F. W. Reuter, H. P. Smith, and J. M. Khan, *Phys. Rev.* **179**, 4 (1969); J. M. Khan, D. L. Potter, and R. D. Worley, *ibid.* **139**, A1735 (1965).

³B. Sellers, F. A. Hanser, and H. H. Wilson, *Phys. Rev.* **182**, 90 (1969).

⁴G. A. Bissinger, J. M. Joyce, E. J. Ludwig, W. S. McEver, and S. M. Shafroth, *Phys. Rev. A* **1**, 841 (1970).

⁵P. Richard, T. I. Bonner, T. Furuta, I. L. Morgan, and J. R. Rhodes, *Phys. Rev. A* **1**, (1970).

⁶L. M. Middleman, R. L. Ford, and R. Hofstadter, *Phys. Rev. A* **2**, 1429 (1970).

⁷CAMAC is a modular instrumentation system for data handling. For a description and specification see Euratom Report No. EUR 4100e, 1969 (unpublished).

⁸G. Huxtable, P. S. Rogers, and F. M. Russell, *Nucl. Instr. Methods* **23**, 357 (1963).

⁹R. D. Dewey, R. S. Mapes, and T. W. Reynolds, in *Progress in Nuclear Energy*, edited by H. A. Eliot and D. C. Stewart (Pergamon, New York, 1969) Ser. 9, Vol. 9.

¹⁰C. M. Lederer, J. M. Hollander, and I. Perlman, *Table of Isotopes* (Wiley, New York, 1968).

¹¹J. L. Campbell, R. J. Goble, and H. J. Smith, *Nucl. Instr. Methods* **82**, 183 (1970).

¹²J. S. Hansen, H. U. Freund, and R. W. Fink, *Nucl. Phys. A* **142**, 604 (1970).

¹³G. S. Khandelwal, B. H. Choi, and E. Merzbacher, *At. Data* **1**, 103 (1969).

¹⁴M. C. Walske, *Phys. Rev.* **101**, 940 (1956).

¹⁵J. D. Garcia, *Phys. Rev. A* **1**, 1402 (1970).

¹⁶J. D. Garcia, *Phys. Rev. A* **1**, 280 (1970); J. D. Garcia, E. Gerjuoy, and J. E. Welker, *Phys. Rev.* **165** 66 (1968).

¹⁷H. Kolbenstvedt, *J. Appl. Phys.* **38**, 4785 (1967). The revised theory was quoted by Middleman *et al.*, Ref. 6.

¹⁸M. Green and V. E. Cosslett, *Proc. Phys. Soc. (London)* **78**, 1206 (1961).

¹⁹O. N. Jarvis, C. Whitehead, and M. Shah, AERE Report No. R 6612, 1970 (unpublished).

PHYSICAL REVIEW A

VOLUME 5, NUMBER 3

MARCH 1972

Multiple-Scattering Expansions for Nonrelativistic Three-Body Collision Problems. VI. Differential and Total Cross Section for Electron-Transfer Rearrangement Collisions*

Joseph C. Y. Chen and Paul J. Kramer[†]

*Department of Physics and Institute for Pure and Applied Physical Sciences,
University of California, San Diego, La Jolla, California 92037*

(Received 24 August 1971)

Differential and total cross sections for electron-transfer rearrangement collisions are calculated in the first-order Faddeev-Watson multiple-scattering approximation for a number of three-body atomic systems. For the (p^+ , H) system, it is shown that the inclusion of the pure p^+-p^+ interaction to all orders (including the contributions coming from the on-shell Coulomb cuts) cancels only part of the effect given by the bare p^+-p^+ interaction so that the present electron-transfer cross section lies in between the Brinkman-Kramers and Jackson-Schiff cross sections and asymptotically approaches the Jackson-Schiff cross section from above in the high-energy limit (where the nonrelativistic approximation is no longer expected to be valid). The knock-out contributions to the electron-transfer amplitude at large angles are particularly important for the equal-mass resonant (e^+ , e^-e^+) electron-transfer collision. Owing to the e^+-e^+ knock-out contribution, the total (e^+ , e^-e^+) electron-transfer cross section exhibits an E^{-3} energy dependence in the high-energy limit.

I. INTRODUCTION

Three-body electron-transfer processes such as

$$p^+ + H \rightarrow H + p^+, \quad (1.1a)$$

$$e^+ + (e^- e^+) \rightarrow (e^+ e^-) + e^+, \quad (1.1b)$$

$$e^+ + H \rightarrow (e^+ e^-) + p^+, \quad (1.1c)$$

$$p^+ + (e^- \mu^+) \rightarrow H + \mu^+ \quad (1.1d)$$

are among the simplest types of rearrangement collision processes. The high-energy behavior of such processes has, however, not yet been adequately understood.¹ The purpose of the present work is to investigate the high-energy behavior of these processes in the first-order Faddeev-Watson multiple-scattering approximation.

One of the difficulties encountered in the past concerns the role of the repulsive pair interaction V_2 [such as the p^+-p^+ interaction in the (p^+ , H) system, for example] in the high-energy behavior of electron-transfer collisions. It is clear that the repulsive interaction may contribute to the electron-transfer amplitude through knock-out collisions

which are peaked in the backward direction. Depending on the particle masses of the system, the knock-out contribution to the electron-transfer amplitude may not always be significant in the energy domain of validity of the nonrelativistic approximation. The repulsive pair interaction may also contribute to the electron-transfer probability through nonclassical behavior. The importance of the nonclassical behavior in the high-energy region depends also on the particle masses of the system. Owing to the large proton-electron mass ratio, one may argue that the (p^+ , H) collision should follow a classical description in the high-energy region. Consequently, the repulsive pair interaction in the (p^+ , H) system (i.e., the p^+-p^+ interaction) merely defines the classical trajectory and introduces a phase factor in the amplitude so that it should not effectively contribute to the (p^+ , H) electron-transfer probability.^{2,3}

Using arguments based on the above classical picture, Brinkman and Kramers³ (BK) neglected the bare p^+-p^+ interaction in their treatment of the (p^+ , H) electron-transfer collision in the first-order